Research Square

Preprints are preliminary reports that have not undergone peer review.
They should not be considered conclusive, used to inform clinical practice,
or referenced by the media as validated information.

# Combining a national-scale grid-based hydrological model with an initial-condition climate ensemble: broad-scale analyses of changes in river flows

**Alison L Kay**

alkay@ceh.ac.uk

UK Centre for Ecology & Hydrology

**Rosanna A Lane**

UK Centre for Ecology & Hydrology

**Nathan Missault**

UK Centre for Ecology & Hydrology

**Wilson CH Chan**

UK Centre for Ecology & Hydrology

**Research Article**

**Keywords:** rainfall-runoff model, seasonal mean flows, floods, droughts, hydro-SMILE

**Posted Date:** November 4th, 2026

**DOI:** https://doi.org/10.21203/rs.3.rs-11291978/v1

**License:** This work is licensed under a Creative Commons Attribution 4.0 International License.
Read Full License

**Additional Declarations:** No competing interests reported.

# Abstract

Climate change alters the hydrological cycle, with changes in river flows and water availability affecting both people and the environment. The typical way to investigate impacts on flows is to drive a hydrological model with climate model ensemble data, where the ensemble is formed by either perturbing the parameters of a single model or using multiple models. But the presence of natural climate variability in each climate model run makes interpretation of differences difficult. Here, a 40-member single-model initial-condition ensemble (SMILE) is used, where each run only varies due to its initialisation. The ensemble members can be considered to represent the range of possibilities from natural climate variability, without being confounded by other differences. A grid-based hydrological model is driven by the climate SMILE, producing 1km grids of monthly mean flows and soil moisture, annual maximum flows, and 7-day annual minimum flows across Great Britain. Broad-scale analyses show clear changes in seasonal mean, high and low flows, which are less noisy when derived from the pooled ensemble than from any individual ensemble member. In particular, the pooled ensemble enables a robust cluster analysis, grouping river pixels across the country by the flow changes they exhibit. Analysis of extreme high and low flows particularly benefits from the far greater sample within the pooled ensemble and seems more robust when then based on empirical distributions rather than fitted extreme value distributions. Better estimation of flow changes from hydrological models driven by SMILEs enables more robust adaptation planning.


# 1. Introduction

Climate change has already caused changes in components of the hydrological cycle, with widespread impacts for both the environment and society (IPCC 2023). Even if mitigation efforts are successful in limiting emissions to net zero over the coming decades, the adverse effects from accumulated emissions will worsen for some time (Palazzo et al. 2023). Changes in occurrence or magnitude of extreme hydrological events (floods and droughts) are one of the main sources of impacts on people and nature (www.unwater.org/water-facts/water-and-climate-change), although general changes in seasonality of the flow regime can also be important, for example affecting water availability, quality and ecology (e.g. Kundzewicz 2008).

Research into the hydrological impacts of climate change in Great Britain (GB) using the latest UK Climate Projections (UKCP18; Lowe et al. 2018) has suggested potentially large decreases in summer and low river flows, and worsening droughts, across the country, with possible increases in winter flows and floods, especially in the north and west (Kay 2021, Lane and Kay 2021, Parry et al. 2024). There is considerable uncertainty related to use of climate models with different parameterisations and/or structures; perturbed-parameter ensembles (PPEs) and multi-model ensembles (MMEs) are commonly used to assess this uncertainty (e.g. Kay 2025, Lane et al. 2026). But each separate run of a climate model also includes natural internal climate variability, which is itself a substantial source of uncertainty (Deser 2020, Jain et al. 2023). Thus when using PPEs and MMEs these different sources of uncertainty are entwined and cannot be easily separated.

Single model initial-condition large ensembles (SMILEs) provide a means to assess the range of uncertainty from internal climate variability, as well as enabling a cleaner estimate of the forced response due the anthropogenic climate change (Deser 2020, Topál et al. 2020, Maher et al. 2021). A SMILE consists of a set of runs of a single climate model, with a fixed parameterisation and the same forcing (future emissions scenario), but with slightly different initialisations. Thus, after an opening period where the 'memory' of the initialisation reduces, the ensemble members can be considered to represent the range of possibilities due to natural climate variability (provided the ensemble size is sufficient; Deser 2020). The ensemble mean (or pooling the ensemble) then gives a better estimate of the forced response, reducing the 'noise' of natural variability because the phasing of internal variability is random between the individual ensemble members (Deser 2020). SMILEs also provide more robust sampling of extreme events and enable estimation of rarer events, due to their provision of significantly more data for each time period which can be readily pooled (Maher et al. 2021, Martel et al. 2020, Brunner et al. 2021). Confounding effects from model structure or parameter differences are avoided, although ideally of course a SMILE would be required for a range of climate models, to more fully assess future impact uncertainty (Deser et al. 2020, Topál et al. 2020).

Maher et al. (2021) provide an overview of various studies using several different types of climate model SMILE. This includes one study using a SMILE to drive a hydrological model; Champagne et al. (2020) investigate future changes in rain-on-snow high flow events in three catchments in southern Ontario using a 50-member SMILE. Poschlod et al. (2020a) use the same SMILE to drive a hydrological model for Bavaria, presenting the impacts of climate change on the amplitude and timing of monthly peaks and troughs in river flows for six flow regime classes. Willkofer et al. (2024) then investigate the impacts on extreme peak flows in Bavaria using the same modelling chain, suggesting that this approach enables more robust estimation of extreme (100-year return period) peak flows using empirical distributions of annual maxima rather than fitting generalized extreme value (GEV) distributions. Similarly, Van der Wiel et al. (2019) compare changes in extreme floods and droughts for several major rivers globally, using a SMILE representing the present-day and 2°C global warming (each with 2000 years of global daily meteorological data) to drive a global hydrological model. They show that fitting a GEV has limitations, especially where the most extreme floods/droughts could have different causes than less extreme ones; use of the empirical distribution derived using a large ensemble avoids those issues. Ehmele et al. (2022) also conclude that use of a large (present-day) climate ensemble with a hydrological model for the Rhine basin provides better estimates for high return period floods than fitting an extreme value distribution, at least for medium/large catchments and provided the climate ensemble is bias-corrected.

The "Climate change in the Arctic-North Atlantic Region and Impacts on the UK" (CANARI) programme produced a SMILE of HadGEM3-GC3.1 — the Global Climate Model (GCM) developed by the UK Met Office, a version of which was also used as the basis for PPEs in UKCP18. Here, the CANARI SMILE is used to drive a national-scale grid-based hydrological model for GB. The modelling chain is described, along with an assessment of performance in the baseline period compared to a run driven by observation-based data. Broad-scale analyses of future changes in flows are then presented, for

simulated annual/seasonal mean flows and for extreme high and low flows, and advantages and limitations are discussed.

## 2. Data and Methods

# 2.1 The national-scale hydrological model

The Grid-to-Grid is a 1km grid-based hydrological model, run at a 15-minute time-step across GB (Bell et al. 2009), with an optional snow-module (Bell et al. 2016). It is not calibrated to individual catchments, instead using spatial datasets (e.g. soil types) to produce a varying response to rainfall inputs in different parts of the country. It performs well across the flow regime for catchments not strongly affected by artificial influences (Rudd et al. 2017, Formetta et al. 2018) — it essentially simulates natural flows.

The model requires driving precipitation and potential evaporation (PE) data, plus temperature data for the snow module. An observation-based run ('Sim_Obs') covers 1969–2022, using i) daily 1km grids of precipitation from HadUK-Grid (Met Office, 2019), divided equally over each time-step; ii) daily 1km grids of PE for short grass derived from HadUK-Grid data (Brown et al. 2023, Robinson et al. 2023), divided equally over each time-step; and iii) daily 1km grids of min and max temperature from HadUK-Grid, interpolated through the day using a sine curve (Kay and Crooks 2014). This model run is initialised using a states file saved at the end of a prior observation-based run covering 1965–1968.

Model outputs include 1km grids of monthly mean flows ($m^3/s$), annual maximum of daily mean flows (AMAX; extracted by water year Oct-Sep, with dates) and annual minimum of 7-day mean flows (AMIN7d; extracted by calendar year, with dates). These are output for 1km 'river pixels', here defined as cells with a contributing area of at least $50km^2$, and are used to investigate potential future changes in river flows across GB (Section 2.3.3). The model also outputs daily mean flow time-series for specific locations corresponding to flow gauging stations, used for the baseline performance analysis (Section 2.3.2). In addition, 1km grids of monthly mean soil moisture (m water / m soil) are output, covering all land cells.

# 2.2 The single model initial-condition large ensemble of a climate model

The CANARI SMILE (hereafter shortened to 'LE') has 40 members, each with the same model parameterisations and forcings but differing by their initial conditions, with a spatial resolution of ~ 60km over the UK (Schiemann et al. 2026b). The initialisation of the 40 members consists of 5 micro perturbations for each of 8 macro perturbations (Schiemann et al. 2026b). The runs are driven by historical forcings for 1950–2014, followed by SSP3-7.0 scenario forcings for 2015–2100. SSP3-7.0 is a relatively high emissions scenario, lower than the highest RCP8.5 emissions scenario used in UKCP18 but still leading to significant global warming, and with other distinctions from other shared socio-

economic pathways (Riahi et al. 2017, Shiogama et al. 2023). For more details on the LE see Schiemann et al. (2026b).

A large set of variables is available from the LE runs (Scheimann et al. 2026a), but the ones relevant here are daily precipitation and min and max temperature, plus the additional variables (e.g. wind speed) required to estimate PE. The latter calculation uses the Hydro-PE method of Robinson et al. (2023), which is based on the UK Met Office's MORECS system (Hough and Jones 1997) and includes an interception component. The Hydro-PE method also allows for adjustment of stomatal resistance under higher $CO_2$ concentrations. Note that the LE data consist of 360-day years, with 12 30-day months.

The precipitation, temperature and PE are bias-adjusted against observation-based data (converted to the GCM-grid scale), using a simple linear scaling approach for temperature and PE but a trend-preserving version of quantile-mapping for precipitation. The bias-adjustments are implemented using the Ibicus python package (Spuler et al. 2024) and are derived using the pooled ensemble, not each ensemble member separately, as it is crucial to maintain the ensemble spread (Ayar et al. 2021, Astagneau et al. 2025). Figure 1 (left) illustrates both raw ('LE_noba') and bias-adjusted ('LE_wba') LE data as the monthly climatology of GB-mean precipitation, min and max temperature, and PE over the historical period, confirming that the bias-adjustments provide a better fit to observed data. This is particularly the case for the seasonal pattern of precipitation. Figure 1 (middle) shows GB-mean timeseries of bias-adjusted LE data overlaid with observations, showing that the latter are within the LE spread. These time-series plots extend to the full period 1950–2099, showing strong increases in temperature and PE, but no clear change in annual total precipitation. However, monthly climatology plots for baseline (1970–1999) and future (2070–2099) periods (Fig. 1 right) show clear summer precipitation decreases and winter precipitation increases, along with increases in summer PE but little change in winter PE, and increases in temperature right through the year.

The bias-adjusted variables are downscaled to 1km, using ratios based on Standard Average Annual Rainfall (SAAR) data for precipitation (Kay et al. 2023), a lapse-rate with altitude for temperature (Bell et al. 2016), but simply copying down the PE (as in Kay 2021). Fig. S1 shows a portion of the GCM grid covering Britain, and the SAAR ratios used for downscaling precipitation in each GCM grid box. To provide the 15-minute inputs required by G2G, the daily precipitation and PE totals are divided equally to the input time-step, and the daily min and max temperature are interpolated through the day using a sine curve, as for observed data (Section 2.1).

Each of the 40 LE members (both without and with bias-adjustment) is used to drive G2G for 1950–2099, with the same state initialisation file in each case, and outputting the same grids as for Sim_Obs along with the daily flow time-series for gauged locations (hereafter 'Sim_LE_noba' and 'Sim_LE_wba'). Simulated data for 1950–1954 are excluded from subsequent analyses, as a spin-up.

# 2.3 Assessment of outputs

# 2.3.1 Analysis of baseline performance

The performance of Sim_LE_noba and Sim_LE_wba in the baseline period is compared against performance of Sim_Obs. The daily flow time-series for locations corresponding to gauged catchments are compared to observed flows from the National River Flow Archive (NRFA; https://nrfa.ceh.ac.uk/), for 644 catchments across GB that have an area greater than 50km$^2$ and less than 20% missing observed data in the period 1971–2010 (Fig. S2a). This analysis cannot directly compare time-step to time-step, as would typically be done, since the LE is free-running (beyond the initial conditions) so is not expected to directly replicate events that actually occurred in the historical period. Instead, distributions of flows are compared (as Kay et al. 2015). Specifically, the fit of three parts of the flow duration curve is assessed; i) lfv_70–95, the percentage bias in lower flow volumes (averaged over the 70-95th quantiles), ii) mdf, the percentage bias in the median flow, and iii) hfv_5–30, the percentage bias in higher flow volumes (averaged over the 5-30th quantiles). These flow duration curve biases are calculated on the square root of flows so there is less emphasis on bias in very high flows. The fit of the flood frequency curve (derived from water-year AMAX as in Section 2.3.2) is also assessed, as the average percentage bias in 2-, 5- and 10-year return period peak flows (ffr). For all four measures, better performance is indicated by values closer to zero.

Given the ~ 60km spatial resolution of the LE data, although the precipitation are spatially downscaled to 1km using patterns of average annual rainfall, the performance for high flows in smaller catchments is a particular concern. To assess the reliability of simulations in smaller catchments, performance is compared for subsets of catchments using a range of minimum thresholds for catchment area between 50 and 400km$^2$. This is used to set a minimum area threshold for the subsequent analysis of future changes in flows, which also focus only on Sim_LE_wba (hereafter ‘Sim_LE’).

## 2.3.2 Analysis of future changes

As an initial broad-scale view of how the Sim_LE outputs evolve over time, GB-mean flow time-series are plotted for 1955–2099, for i) annual mean flows (derived from the monthly mean flow grids), ii) AMAX flows and iii) AMIN7d flows. The monthly climatology of GB-mean flows for 1970–1999 and 2070–2099 are also derived from the monthly mean flow grids. In addition, GB-mean annual mean soil moisture, and the monthly climatology of soil moisture for 1970–1999 and 2070–2099, are derived from the monthly mean soil moisture grids, to provide context for flow changes. In each case, the equivalents from Sim_Obs (1969–2022) are shown for comparison. Trend analyses are performed for an overlapping period of Sim_Obs and the historical portion of Sim_LE (1969–2014), as well as for the full Sim_LE period (1955–2099). A simple linear trend line is fitted to the annual time-series in each case, with the slope used as the trend size. To demonstrate the range of natural variability in both Sim_LE and Sim_Obs, trend lines are also fitted to each continuous 30-year period within 1969–2014 and the distribution of these slopes shown, with kernel density estimators. This and subsequent analyses only include pixels with a contributing area above the threshold defined by the baseline performance analysis.

The Sim_LE outputs are then used to investigate changes in flows for six regions of GB, using running 30-year periods from 1955–1984 until 2070–2099, moving forward 5 years at a time, relative to a

baseline derived using the pooled ensemble for 1970–1999. Using a baseline derived from the pooled ensemble provides a more consistent comparison between ensemble members, from a more representative baseline. The monthly mean river flow grids are used to investigate changes in seasonal mean flows for the four standard seasons (Winter, Dec-Feb; Spring, Mar-May; Summer, Jun-Aug; Autumn, Sep-Nov). The simulated AMAX and AMIN7d grids are used to investigate changes in high and low flows respectively, initially focussing on the 10-year return period (RP) by fitting an extreme value distribution (GLO for AMAX and GEV for AMIN7d; as Kay 2025) to data for each river pixel for each 30-year time-slice. Note that, since the AMAX extraction uses water years (Sep-Oct), there are small (3-month) offsets in the 30-year periods used for this analysis, relatively to the time-slices listed above.

For each of the six flow indices above the calculations are done for each ensemble member separately, as well as pooling the data together. For example, for the 30 water-years Oct 2010-Sep 2040, at each river pixel there are 30 AMAX for each ensemble member, but the data from the 40 ensemble members can be pooled to give 1200 AMAX for the 30-year period at each river pixel. For the pooled ensemble, higher RP high and low flows are then investigated, comparing results from the fitted extreme value distributions with use of empirical distributions of AMAX and AMIN7d respectively.

Pixel-based changes in the six flow indices are averaged across six regions (Fig. S2b), derived by combining UKCP18 river-basin regions (Met Office Hadley Centre 2019). The combination of regions is based on prior knowledge of typical west/east and north/south differences in flow regimes and climate change impacts on flows, but the choice inevitably represents a balance between showing regional differences without too many plots.

To investigate differences that may occur even on sub-regional scales, a cluster analysis is performed on time-series of pixel-based flow changes derived from the pooled ensemble (not for each ensemble members separately). This looks at mean flows for the four seasons, as well as 10- and 100- year RP high and low flows (derived using both empirical and fitted extreme value distributions). The time-series from the pooled ensemble are less noisy, making it easier for the cluster analysis to identify and group time-series that are evolving similarly. The analysis applies k-means clustering with the Euclidean distance metric (implemented using the python library tslearn, Tavenard et al. 2020), deriving 5 clusters for each flow index (determined from elbow plots testing cluster sizes from 2 to 12).

## 3. Results

# 3.1 Analysis of baseline performance

Figure 4 (left) summarises the performance of Sim_LE with and without bias-adjustment (Sim_LE_wba and Sim_LE_noba respectively) relative to Sim_Obs, across 644 catchments, for the four measures described in Section 2.3.1. It shows that the bias-adjustments have brought the performance of Sim_LE back towards that of Sim_Obs, as expected. In particular, the range of Sim_LE_noba performance is

wider than Sim_Obs, with the range of Sim_LE_wba reduced back towards that of Sim_Obs. The median performance of Sim_LE_wba is also generally closer to that of Sim_Obs.

Figure 4 (left) also shows how performance varies as a gradually increasing area threshold is imposed on the set of catchments included. Performance varies relatively little with area for low flow volume (lfv_70–95), median flow (mdf) and high flow volume (hfv_5–30), but gradually improves for peak flows (ffr) as smaller catchments are excluded. Plots of the difference in performance between Sim_LE_wba and Sim_Obs (Fig. 4 right) suggest that the area threshold with the least difference in performance is 200km$^2$. This threshold is used for subsequent analyses of gridded flows, which also focus on the simulations driven by the bias-adjusted version of the LE data, Sim_LE_wba, hereafter termed Sim_LE.

# 3.2 Analysis of future changes

# 3.2.1 GB-mean flows and soil moisture

GB-mean time-series of flows and soil moisture (Fig. 3) show a good correspondence between Sim_LE and Sim_Obs. The range from the former encompasses the latter for each variable, and the standard deviation of the time-series from Sim_Obs sits within the range of that from Sim_LE for the overlapping historical period (1969–2014) for each (see Table S1). The trends for the mean of Sim_LE for each variable over the full period (1955–2099) are all highly statistically significant (significant at the 1% level), and for the shorter historical period (1969–2014) the trends are also highly significant for all variables expect annual maximum flows, where the trend is not significant (even at the 20% level).

The Sim_LE annual mean flow time-series show a relatively small decrease over 1955–2099 (-0.0143 m$^3$/yr for the Sim_LE mean), with a similar magnitude trend for the overlapping historical period (-0.0164 m$^3$/yr for the Sim_LE mean), but the spread of trends across ensemble members in the shorter period is much larger than for the full period. Although Sim_Obs shows a contrasting increasing trend in annual mean flows over the historical period (+ 0.0632 m$^3$/yr, significant at the 5% level), it is just within the range from the Sim_LE; one ensemble member shows a slightly higher trend over that period. The monthly climatology plots show that the flow reductions in Sim_LE mainly occur in summer and autumn, with some increases in winter months.

The Sim_LE annual soil moisture times-series show a clearer decrease over 1955–2099 compared to annual mean flows, with the monthly climatology plots showing greater summer and autumn drying and no clear winter wetting. The trend of the Sim_LE mean over 1955–2099 (-0.000242 units/yr) is slightly larger magnitude (more negative) than that over 1969–2014 (-0.000189 units/yr), although again the spread of trends across ensemble members in the shorter period is much larger. As for annual mean flows, Sim_Obs shows a contrasting increasing trend over the historical period (+ 0.000158 units/yr, not significant), but this is just within the range of the Sim_LE members.

The Sim_LE AMAX times-series show a relatively small increase over 1955–2099 (+ 0.107 m$^3$/yr for the Sim_LE mean), but in the historical period the ensemble mean trend is near zero (+ 0.025m$^3$/yr, not

significant), with members spread both sides of zero. As for annual mean flows and soil moisture, the trend from Sim_Obs (+ 0.554 $m^3$/yr, significant at the 5% level) sits towards the top end of the range from Sim_LE over the historical period.

The Sim_LE AMIN7d time-series shows a clear decrease over both 1955–2099 (-0.0119 $m^3$/yr for the Sim_LE mean) and 1969–2014 (-0.00895 $m^3$/yr for the Sim_LE mean), although again the Sim_Obs trend sits towards the top end of the range from the Sim_LE members, with a trend that is actually positive (+ 0.00989 $m^3$/yr, only significant at the 20% level).

For all four variables, plots of the distribution of trend sizes from each continuous 30-year sub-period within 1969–2014 show a wide range of values, illustrating the strong influence of natural variability over shorter periods. While there is a lot of overlap between these distributions for Sim_LE and Sim_Obs, the latter generally sits towards higher trend values than the former. Regional-mean flow changes

Time-series of regional mean flow changes (Fig. 4), using a 30-year window moved forward 5 years at a time, show some clear differences across the country. In regions to the north and west there are generally increases in winter, a mixed pattern of increases/decreases in spring, and mostly decreases in summer and autumn, whereas in the south-east there are mostly decreases throughout the year. There are generally increases in 10-year return period high flows, although after an initial decrease in the south-east. There are strong decreases in 10-year return period low flows for all regions. The individual ensemble members show the same overall trends but with high variability compared to the pooled ensemble, particularly in spring and for 10-year return period high flows.

Using the pooled ensemble, high/low flow changes are derived for a range of return periods using the empirical distribution and the fitted extreme value distribution (Fig. 5). These are very similar to each other for lower return periods (up to ~ 50 years), as would be expected, but can differ substantially for higher return periods, indicating potential issues with the fitting of extreme value distributions. For more extreme low flows, the changes derived from fitted distributions decrease more than those from the empirical distributions. They are also more ‘noisy’, indicating how much the inclusion/exclusion of certain extreme values can affect the fit as the 30-year window is moved through time. Interestingly, for more extreme high flows, the changes derived from both fitted and empirical distributions seem to suffer from some ‘noise’ as the 30-year window is moved through time, although they still generally track each other relatively closely.

# 3.2.2 Cluster-analysis of pixel-based flow changes

Results from the cluster analysis of pixel-based flow changes from the pooled ensemble reveal differing spatial patterns for different flow indices (Fig. 6). For seasonal mean flows, there is a more west/east gradient of changes for winter and spring (increases in the west and decreases in the east), a more north/south gradient for summer (lesser decreases to the north and greater decreases to the south), and

a more north/west to south/east gradient for autumn (increases to the north/west and decreases to the south/east).

The spatial pattern of changes in 10-year return period high flows looks similar to that for winter, although the pattern for 100-year return period high flows in less clear. The spatial pattern of changes in both 10- and 100-year return period low flows looks relatively similar to that for summer, although the changes themselves are much more pronounced. In each case there are also smaller scale variations which reflect catchment properties, particularly the presence of a significant groundwater component in parts of England (cf. Kay et al. 2021).

The empirical distributions are used for the high and low flow changes in Fig. 6, but equivalent plots derived using extreme value distributions are shown in Fig. S3. These illustrate a particular issue with the fitted distributions for low flows, which show a lot of instability for some pixels as the 30-year window is moved through time.

# 4. Discussion

A major advantage of single-model initial-condition large climate ensembles (SMILEs) is that they significantly increase the amount of data available for historical and future climates, without the confounding effect of model structure or parameter differences related to MMEs or PPEs. Thus the data can be readily pooled, reducing the noise from natural variability which occurs on a range of time-scales (e.g. from the seasonal up-to decadal variations of the North Atlantic Oscillation, and the Atlantic Multidecadal Oscillation; climate.metoffice.cloud/climate_modes.html). This is equally the case when SMILEs are used to drive hydrological models; the flow analyses presented here show much cleaner changes in flows over the 21st century from the pooled ensemble (or the ensemble mean) than from any individual ensemble member. The analysis also highlights the fact that the actual evolution of the historical observed climate, and thus river flows, was only one possibility out of a wide range that could have occurred. Chan et al. (2025) used a different SMILE to drive a catchment-based hydrological model for 190 catchments across Britain. The resulting hydro-SMILE shows both wetting and drying trends could have occurred over a historical period, which provides context for the observed trend and helps to explain a perceived inconsistency between recent observations and longer-term climate projections. Here, the Sim_Obs trends sit towards higher values than those from Sim_LE in the historical period (Fig. 3), which could be because what actually occurred over 1969–2014 was more dominated by certain patterns of natural variability, whereas the LE is sufficiently large that it should represent the full range of what could have occurred historically. However, it could also be because the climate model is not sufficiently capturing natural variability that may occur on longer time scales, or, more concerningly, is not capturing an important element of forced response due to anthropogenic emissions. These issues are discussed by Blackport and Fyfe (2022), in terms of similar discrepancies for trends in precipitation (and the Jet Stream) between climate models and observations.

When considering extreme flows, the much larger sample size from hydro-SMILEs provides the further advantage of enabling estimation of flows for much higher return periods than would typically be recommended using annual maxima or minima from a 30-year period. In addition, a possible advantage is enabling the use of empirical distributions, rather than requiring the fitting of extreme value distributions. One situation where this is particularly beneficial is if a river dries up at times in future, leading to some annual minima being zero; empirical distributions can deal with this much more easily than fitted distributions. For high flows, it is possible that the most extreme floods have different causes than less extreme ones (e.g. compound events), therefore it may not be expected that one extreme value distribution will fit both well (Van der Wiel et al. 2019). Willkofer et al. (2024), Ehmele et al. (2022) and Van der Wiel et al. (2019) suggest that use of empirical distributions is preferable to fitting extreme value distributions when large samples are available. For extreme precipitation, Wehner et al. (2024) suggest that it is still worth fitting extreme value distributions to reduce uncertainty in estimating long-period return values, even for very large ensembles, "provided the assumptions underlying GEV theory are appropriate"; the latter proviso is clearly key. Better estimation of extremes from the much larger sample of events from hydro-SMILEs enables more robust adaptation planning.

One limitation of the current study is the use of only one SMILE, based on the Met Office Hadley Centre GCM. Projections from this GCM can be quite different to those from other GCMs, in particular projecting greater future decreases in summer precipitation (Short and Kendon 2024). Ideally multiple SMILEs would be applied, to enable a fuller picture of potential future changes in climate, and thus river flows when used to produce hydro-SMILEs, but this would be a large undertaking which is not yet possible. Furthermore, the ~ 60km resolution of the GCM is relatively coarse for hydrological modelling over Britain, where even the largest catchments only have drainage areas of the order of 10,000km$^2$; ~3 GCM grids boxes. Precipitation from the GCM has been spatially downscaled to 1km based on historical patterns, and this is expected to improve the flow simulations compared to direct use of the coarse data, but there are likely still differences compared to use of 1km data, were it available (Kay et al. 2023). This is particularly the case for high flows, where the spatial (and temporal) variation of inputs is more important than for low flows, and is why an area threshold was selected so that smaller catchments were excluded from subsequent analyses. Future work will look at events from the LE dynamically downscaled using nested finer-resolution Regional and Convection-Permitting models (RCMs/CPMs) and investigate how this affects subsequent flow simulations.

A further limitation of the current study is the use of a single emissions scenario; SSP3-7.0. This was chosen following criticisms that the highest emissions scenario RCP8.5, frequently used in previous studies (e.g. UKCP18, Murphy et al. 2018), was now considered unrealistically large (Arnell et al. 2021b, Shiogama et al. 2023). But the second highest emissions scenario, SSP3-7.0, has other key differences which will affect climate simulations driven by it and may need to be considered to enable proper interpretation of derived results (Shiogama et al. 2023). It also means that it is difficult to compare results from this study with those from previous studies based on UKCP18 RCM data for example. Use of time-scaling, whereby future time-periods are compared based on equivalence of the global mean surface temperature change reached, rather than using fixed future periods across different climate

model runs, is one possible way to enable comparison between studies (e.g. Arnell et la. 2021a, Kay 2025), but may not fully account for the differences in the definition of the SSP3-7.0 emissions scenario.

Finally, only one hydrological model has been applied here. Previous work has suggested that, while the choice of hydrological model may not be so important for the study of high flows it can be more important for low flows (e.g. Giuntoli et al. 2015, De Niel et al. 2019). A range of catchment-based hydrological models are being used with the CANARI LE data; results using these will be reported elsewhere (Chan et al., in prep.).

# 5. Conclusions

Each separate run of a climate model includes uncertainty from natural climate variability, which is combined with model uncertainty when using multi-model or perturbed-parameter climate model ensembles (e.g. from EuroCORDEX or UKCP18). Single model initial-condition large ensembles (SMILEs), where only the initialisation (not the model structure or parameterisation) varies between runs, i) allow assessment of the range of uncertainty from internal climate variability, ii) enable a cleaner estimate of the forced response, and iii) provide more robust sampling of extreme events from pooled data. These advantages carry through to model simulations driven by climate SMILEs, like hydro-SMILEs produced using hydrological models.

Here, a grid-based hydrological model for Great Britain has been driven by a climate SMILE of the Hadley Centre Global Climate Model, producing 1km grids of monthly mean river flows, monthly mean soil moisture, annual maximum flows, and 7-day annual minimum flows. Subsequent broad-scale analyses show clear changes in the seasonal pattern of flows, high flows and low flows, which are cleaner when derived from the pooled ensemble than from any individual ensemble member. Changes vary regionally. Analysis of extreme high and low flow changes seems to be more robust when based on the pooled ensemble and empirical distributions, rather than fitted extreme value distributions.

Further work will look in more detail at variations in response between catchments. In particular, flood analyses will use dynamically-downscaled events selected from the GCM SMILE; being both higher spatial and temporal resolution, these data should enable improved simulation of high flows compared to the relatively coarse GCM data. Drought analyses will make use of the large sample size to sample for record-breaking events that could complement existing risk planning methodologies to stress-test water resources systems (e.g. Chan et al. 2023). The SMILE will also enable investigation of rare but potentially highly impactful compound events, the rarity of which makes them particularly difficult to study using limited periods of observational data (e.g. Poschlod et al. 2020b, Bevaqua et al. 2023, Lehner 2024).

# Declarations

# Author Contribution

AK ran the hydrological model, performed the flow analyses, wrote the draft manuscript and finalised the manuscript. RL, NM and WC pre-processed and checked data for running the hydrological model (including making PE and testing/applying bias-adjustment). All authors reviewed the final manuscript.

# Acknowledgements

This work was supported by the Natural Environment Research Council award number NE/W004984/1 (CANARI).

# Data Availability

The CANARI LE data (priority variables) are available from https://catalogue.ceda.ac.uk/uuid/4b62fafc68ae4c3784fb2819f652c537/. The simulated flow data are available from the author upon reasonable request.

## References

1. Arnell NW, Freeman A, KAY AL, Rudd AC, Lowe JA (2021a) Indicators of climate risk in the UK at different levels of warming. Environ Res Commun 3(9):095005. 10.1088/2515-7620/ac24c0
2. Arnell NW, Kay AL, Freeman A, Rudd AC, Lowe JA (2021b) Changing climate risk in the UK: a multi-sectoral analysis using policy relevant indicators. Clim Risk Manage 31:100265. 10.1016/j.crm.2020.100265
3. Astagneau PC, Wood RR, Vrac M, Kotlarski S, Vaittinada Ayar P, François B, Brunner MI (2025) Impact of bias adjustment strategy on ensemble projections of hydrological extremes. Hydrol Earth Syst Sci 29(20):5695–5718. 10.5194/hess-29-5695-2025
4. Ayar PV, Vrac M, Mailhot A (2021) Ensemble bias correction of climate simulations: preserving internal variability. Sci Rep 11:3098. 10.1038/s41598-021-82715-1
5. Bell VA, Kay AL, Davies HN, Jones RG (2016) An assessment of the possible impacts of climate change on snow and peak river flows across Britain. Clim Change 136(3):539–553. 10.1007/s10584-016-1637-x
6. Bell VA, Kay AL, Jones RG, Moore RJ, Reynard NS (2009) Use of soil data in a grid-based hydrological model to estimate spatial variation in changing flood risk across the UK. J Hydrol 377(3–4):335–350. 10.1016/j.jhydrol.2009.08.031
7. Bevacqua E, Suarez-Gutierrez L, Jézéquel A et al (2023) Advancing research on compound weather and climate events via large ensemble model simulations. Nat Commun 14:2145. 10.1038/s41467-023-37847-5
8. Blackport R, Fyfe JC (2022) Climate models fail to capture strengthening wintertime North Atlantic jet and impacts on Europe. Sci Adv 8:eabn3112. 10.1126/sciadv.abn3112

9. Brown MJ, Robinson EL, Kay AL, Chapman R, Bell VA, Blyth EM (2023) Potential evapotranspiration derived from HadUK-Grid 1km gridded climate observations 1969–2022 (Hydro-PE HadUK-Grid). https://doi.org/10.5285/beb62085-ba81-480c-9ed0-2d31c27ff196. NERC EDS Environmental Information Data Centre
10. Brunner MI, Swain DL, Wood RR et al (2021) An extremeness threshold determines the regional response of floods to changes in rainfall extremes. Commun Earth Environ 2:173. 10.1038/s43247-021-00248-x
11. Champagne O, Leduc M, Coulibaly P, Arain MA (2020) Winter hydrometeorological extreme events modulated by large-scale atmospheric circulation in southern Ontario. Earth Syst Dynam 11:301–318. 10.5194/esd-11-301-2020
12. Chan WCH, Arnell NW, Darch G, Facer-Childs K, Shepherd TG, van der Tanguy M (2023) Current and future risk of unprecedented hydrological droughts in Great Britain. J Hydrol 625:130074. :/10.1016/j.jhydrol.2023.130074
13. Chan W, Tanguy M, Chevuturi A, Hannaford J (2025) Climate variability conceals emerging hydrological trends across Great Britain. J Hydrol, 660(A),133414.
14. Chan W, Missault N, Lane RA, Kay AL, Chevuturi A, Hannaford J (in prep.). New insights on UK hydrological extremes using a large initial-condition climate ensemble
15. De Niel J, Van Uytven E, Willems P (2019) Uncertainty Analysis of Climate Change Impact on River Flow Extremes Based on a Large Multi-Model Ensemble. Water Resour Manage 33:4319–4333. 10.1007/s11269-019-02370-0
16. Deser C (2020) Certain uncertainty: The role of internal climate variability in projections of regional climate change and risk management. Earths Future. 8, e2020EF001854 10.1029/2020EF001854
17. Deser C, Lehner F, Rodgers KB et al (2020) Insights from Earth system model initial-condition large ensembles and future prospects. Nat Clim Chang 10:277–286. 10.1038/s41558-020-0731-2
18. Ehmele F, Kautz L-A, Feldmann H, He Y, Kadlec M, Kelemen FD, Lentink HS, Ludwig P, Manful D, Pinto JG (2022) Adaptation and application of the large LAERTES-EU regional climate model ensemble for modeling hydrological extremes: a pilot study for the Rhine basin. Nat Hazards Earth Syst Sci 22(2):677–692. 10.5194/nhess-22-677-2022
19. Formetta G, Prosdocimi I, Stewart E, Bell V (2018) Estimating the index flood with continuous hydrological models: an application in Great Britain. Hydrol Res 49:123–133, doi:10. 2166/nh. 2017. 251
20. Giuntoli I, Vidal J-P, Prudhomme C, Hannah DM (2015) Future hydrological extremes: the uncertainty from multiple global climate and global hydrological models. Earth Syst Dynam 6:267–285. 10.5194/esd-6-267-2015
21. Hough MN, Jones RJA (1997) The United Kingdom meteorological office rainfall and evaporation calculation system: MORECS version 2.0-an overview. Hydrol Earth Syst Sci 1:227–239
22. IPCC (2023) Summary for Policymakers. In: Lee H, Romero J (eds) Climate Change 2023: Synthesis Report. Contribution of Working Groups I, II and III to the Sixth Assessment Report of the

Intergovernmental Panel on Climate Change [Core Writing Team. IPCC, Geneva, Switzerland, pp 1–34. doi: 10.59327/IPCC/AR6-9789291691647.001.

23. Jain S, Scaife AA, Shepherd TG et al (2023) Importance of internal variability for climate model assessment. npj Clim Atmos Sci 6:68. 10.1038/s41612-023-00389-0
24. Kay AL (2021) Simulation of river flow in Britain under climate change: baseline performance and future seasonal changes. Hydrol Process 35(4):e14137. 10.1002/hyp.14137
25. Kay AL (2025) A comparison of hydrological impacts from two ensembles of regional climate projections with a range of climate sensitivities. Reg Environ Change 25:89. 10.1007/s10113-025-02426-5
26. Kay AL, Crooks SM (2014) An investigation of the effect of transient climate change on snowmelt, flood frequency and timing in northern Britain. Int J Climatol 34(12):3368–3381. 10.1002/joc.3913
27. Kay AL, Griffin A, Rudd AC, Chapman RM, Bell VA, Arnell NW (2021) Climate change effects on indicators of high and low river flow across Great Britain. Adv Water Resour 151:103909. 10.1016/j.advwatres.2021.103909
28. Kay AL, Rudd AC, Coulson J (2023) Spatial downscaling of precipitation for hydrological modelling: assessing a simple method and its application under climate change in Britain. Hydrol Process 37(2):e14823. 10.1002/hyp.14823
29. Kay AL, Rudd AC, Davies HN, Kendon EJ, Jones RG (2015) Use of very high resolution climate model data for hydrological modelling: baseline performance and future flood changes. Clim Change 133(2):193–208. 10.1007/s10584-015-1455-6
30. Kundzewicz ZW (2008) Climate change impacts on the hydrological cycle. Ecohydrol Hydrobiol 8(2–4):195–203. 10.2478/v10104-009-0015-y
31. Lane RA, Kay AL (2021) Climate change impact on the magnitude and timing of hydrological extremes across Great Britain. Front Water 3:684982. 10.3389/frwa.2021.684982
32. Lane RA, Rudd AC, Kay AL (2026) Climate change impact on hydrological droughts: differences between two ensembles of regional climate projections across Great Britain. J Hydrology: Reg Stud 65:103417. 10.1016/j.ejrh.2026.103417
33. Lehner F (2024) Climate model large ensembles as test beds for applied compound event research. iScience 27(11):111113. 10.1016/j.isci.2024.111113
34. Lowe JA, Bernie D et al (2018) UKCP18 science overview report. Met Office Hadley Centre
35. Maher N, Milinski S, Ludwig R (2021) Large ensemble climate model simulations: introduction, overview, and future prospects for utilising multiple types of large ensemble. Earth Syst Dynam 12:401–418. 10.5194/esd-12-401-2021
36. Martel JL, Mailhot A, Brissette F (2020) Global and regional projected changes in 100-yr subdaily, daily, and multiday precipitation extremes estimated from three large ensembles of climate simulations. J Clim 33(3):1089–1103. 10.1175/JCLI-D-18-0764.1

37. Met Office Hadley Centre (2019) UKCP18 Guidance: Data availability, access and formats. https://www.metoffice.gov.uk/binaries/content/assets/metofficegovuk/pdf/research/ukcp/ukcp18-guidance-data-availability-access-and-formats.pdf
38. Met Office, Hollis D et al (2019) Had UK-Grid Gridded Climate Observations on a 1km grid over the UK, v1.0.0.0 (1862–2017). Centre for Environmental Data Analysis, November 2019. 10.5285/2a62652a4fe6412693123dd6328f6dc8
39. Murphy JM, Harris GR, Sexton DMH, Kendon EJ, Bett PE, Clark RT, Eagle KE, Fosser G, Fung F, Lowe JA, McDonald RE, McInnes RN, McSweeney CF, Mitchell JFB, Rostron JW, Thornton HE, Tucker S, Yamazaki K (2018) UKCP18 land projections: Science report. Met Office Hadley Centre
40. Palazzo Corner S, Siegert M, Ceppi P, Fox-Kemper B, Frölicher TL, Gallego-Sala A, Haigh J, Hegerl GC, Jones CD, Knutti R, Koven CD, MacDougall AH, Meinshausen M, Nicholls Z, Sallée JB, Sanderson BM, Séférian R, Turetsky M, Williams RG, Zaehle S, Rogelj J (2023) The Zero Emissions Commitment and climate stabilization. Front Sci 1:1170744. 10.3389/fsci.2023.1170744
41. Parry S, Mackay JD, Chitson T, Hannaford J, Magee E, Tanguy M, Bell VA, Facer-Childs K, Kay A, Lane R, Moore RJ, Turner S, Wallbank J (2024) Divergent future drought projections in UK river flows and groundwater levels. Hydrol Earth Syst Sci 28(3):417–440. 10.5194/hess-28-417-2024
42. Poschlod B, Willkofer F, Ludwig R (2020a) Impact of climate change on the hydrological regimes in Bavaria, Water, 12, 1599. 10.3390/w12061599
43. Poschlod B, Zscheischler J, Sillmann J, Wood RR, Ludwig R (2020b) Climate change effects on hydrometeorological compound events over southern Norway. Weather Clim Extremes 28:100253
44. Riahi K, van Vuuren DP, Kriegler E et al (2017) The Shared Socioeconomic Pathways and their energy, land use, and greenhouse gas emissions implications: An overview. Glob Environ Change 42:153–168. 10.1016/j.gloenvcha.2016.05.009
45. Robinson EL, Brown MJ, Kay AL, Lane RA, Chapman R, Bell VA, Blyth EM (2023) Hydro-PE: gridded datasets of historical and future Penman–Monteith potential evaporation for the United Kingdom. Earth Syst Sci Data 15:4433–4461. 10.5194/essd-15-4433-2023
46. Rudd AC, Bell VA, Kay AL (2017) National-scale analysis of simulated hydrological droughts (1891–2015). J Hydrol 550:368–385, doi:10. 1016/j. jhydr ol. 2017. 05. 018
47. Schiemann RKH, Lister G, Hatcher R, Hodson D, Lawrence B, Shaffrey LC, Cole J, Dittus A, Mecking J, Robson J, Wilson S, Aksenov Y, Blaker A, Harvey B, Martinez-Alvarado O, Osprey A, Rynders S, Ahmadi S, Aylmer J, Baker L, Case D, Gentile ES, George S, Hodges K, Karlowska E, Lang C, Lu H, O'Callaghan N, Osmolska W, Osprey S, Phillips T, Schröder D, Smith R, Turner AG, Woolnough S, Andrews M, Coward A, Hardiman S, Harle J, Rostron J, Sexton D, Sinha B, Williams J, Wilson C (2026a): CANARI LE Priority Variables from the HadGEM3.1 large ensemble of climate model simulations for the CANARI project (v1). NERC EDS Centre for Environmental Data Analysis, 04 September 2026. 10.5285/4b62fafc68ae4c3784fb2819f652c537. https://dx.doi.org/10.5285/4b62fafc68ae4c3784fb2819f652c537

48. Schiemann RKH, Lister G, Hatcher R, Hodson D, Lawrence B, Shaffrey L, Cole J, Dittus A, Mecking J, Robson J, Wilson S, Aksenov Y, Blaker AT, Harvey B, Martínez-Alvarado O, Osprey A, Rynders S, Ahmadi S, Aylmer J, Baker L, Case D, Gentile ES, George S, Hodges K, Karlowska E, Lang C, Lu H, O'Callaghan N, Osmolska W, Osprey S, Phillips T, Schröder D, Smith R, Turner AG, Woolnough S, Andrews M, Coward A, Hardiman S, Harle J, Rostron JW, Sexton DMH, Sinha B, Williams J, Wilson C (2026b) The CANARI HadGEM3 Large Ensemble: Design, and evaluation of historical experiments. EGUsphere [preprint] https://doi.org/10.5194/egusphere-2026-2281
49. Shiogama H, Fujimori S, Hasegawa T et al (2023) Important distinctiveness of SSP3–7.0 for use in impact assessments. Nat Clim Chang 13:1276–1278. 10.1038/s41558-023-01883-2
50. Short C, Kendon L (2024) Augmenting UKCP Local (2.2km) projections by down-scaling global models from CMIP5. Report from UK Met Office Hadley Centre, November 2024
51. Spuler FR, Wessel JB, Comyn-Platt E, Varndell J, Cagnazzo C (2024) ibicus: a new open-source Python package and comprehensive interface for statistical bias adjustment and evaluation in climate modelling (v1.0.1). Geosci Model Dev 17:1249–1269. 10.5194/gmd-17-1249-2024
52. Tavenard R, Faouzi J, Vandewiele G, Divo F, Androz G, Holtz C, Payne M, Yurchak R, Russwurm M, Kolar K, Woods E (2020) Tslearn, A Machine Learning Toolkit for Time Series Data. J Mach Learn Res 21(118):1–6
53. Topál D, Hatvani IG, Kern Z (2020) Refining projected multidecadal hydroclimate uncertainty in East-Central Europe using CMIP5 and single-model large ensemble simulations. Theor Appl Climatol 142:1147–1167. 10.1007/s00704-020-03361-7
54. Van der Wiel K, Wanders N, Selten FM, Bierkens MFP (2019) Added value of large ensemble simulations for assessing extreme river discharge in a 2 ∘C warmer world. Geophys Res Lett 46:2093–2102. 10.1029/2019GL081967
55. Wehner MF, Duffy ML, Risser M, Paciorek CJ, Stone DA, Pall P (2024) On the uncertainty of long-period return values of extreme daily precipitation. Front Clim 6:1343072. 10.3389/fclim.2024.1343072
56. Willkofer F, Wood RR, Ludwig R (2024) Assessing the impact of climate change on high return levels of peak flows in Bavaria applying the CRCM5 large ensemble. Hydrol Earth Syst Sci 28(13):2969–2989. 10.5194/hess-28-2969-2024

# Figures

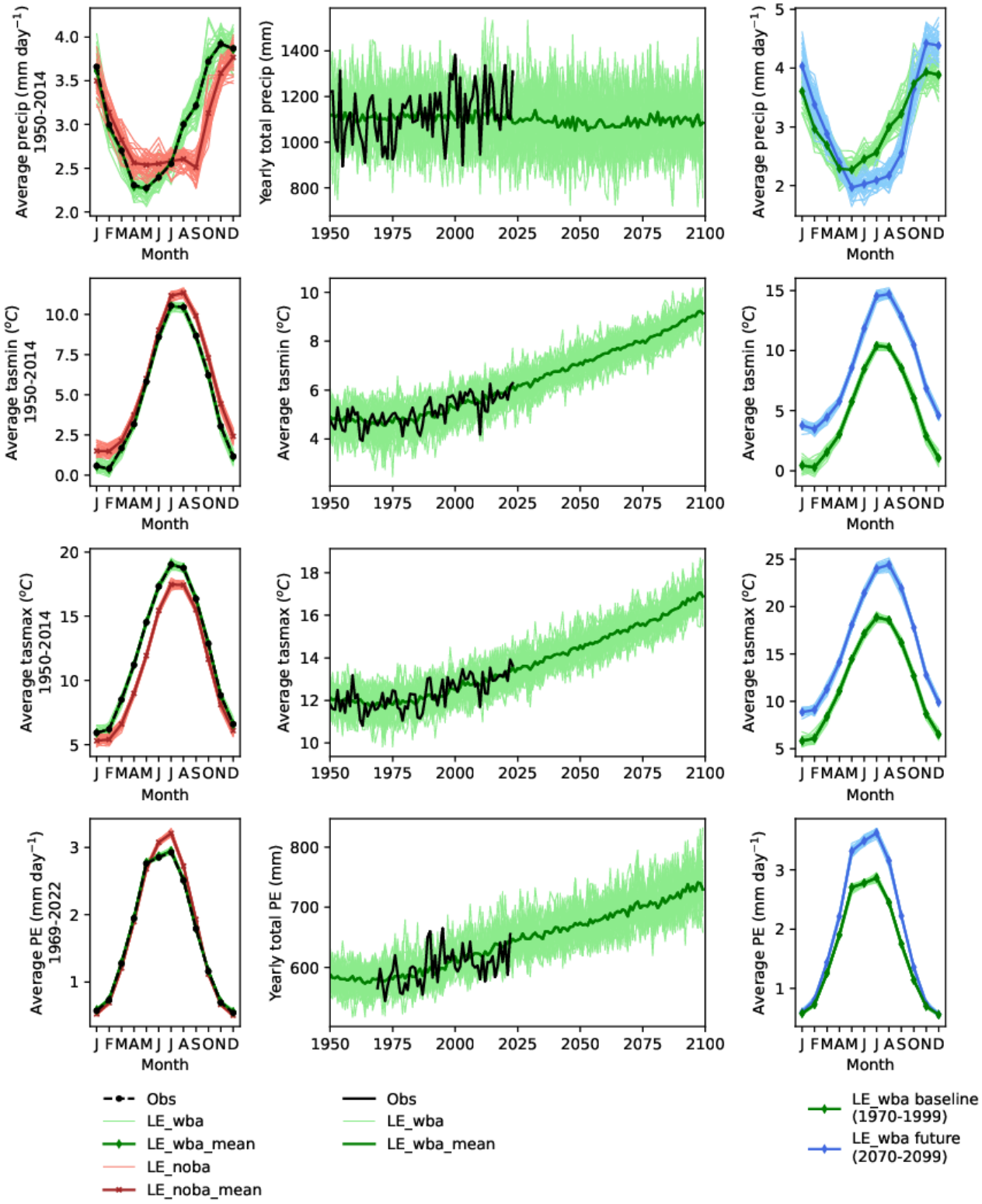



**Figure 1**

Plots of GB-mean precipitation, temperature and PE, demonstrating trends and biases in the LE. The left column shows precipitation (top row), min/max temperature (middle rows) and PE (bottom row) monthly climatology over the bias adjustment period, comparing the LE with and without bias adjustment (green/red lines respectively) to observations (black dashed line). Thin lines indicate each ensemble member, and bold lines show the ensemble mean. The middle column shows time-series of GB-mean

yearly values for each variable, including the bias adjusted LE output (green lines) and observations (black line). The right column shows monthly climatology over the baseline (green) and future (blue) periods across all ensemble members (thin lines) and the ensemble mean (bold lines).

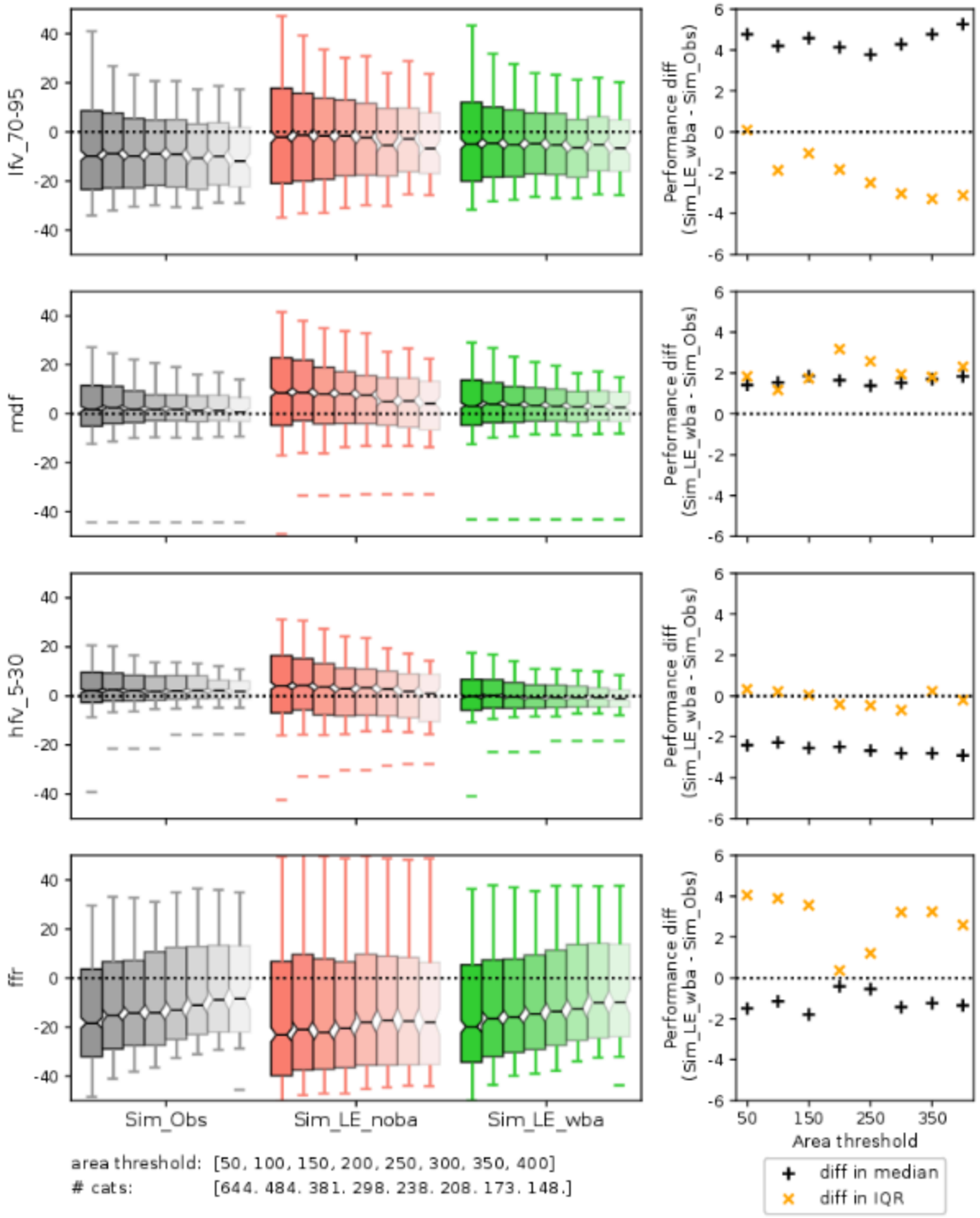



**Figure 2**

Summary of performance of Sim_LE_noba and Sim_LE_wba vs Sim_Obs (left), for the four performance measures (top-to-bottom), for 644 catchments across GB (first boxplot in each case). Subsequent

boxplots show the performance for gradually increasing area thresholds above 50km$^2$, increasing by 50km$^2$ at a time up to 400km$^2$. The number of catchments remaining for each area threshold is indicated by the text underneath the boxplots. Also shown (right) is the difference in performance between Sim_LE_wba and Sim_Obs, plotted as the difference in the median (plus signs) and the difference in the interquartile range (crosses) for each threshold and each of the four performance measures.

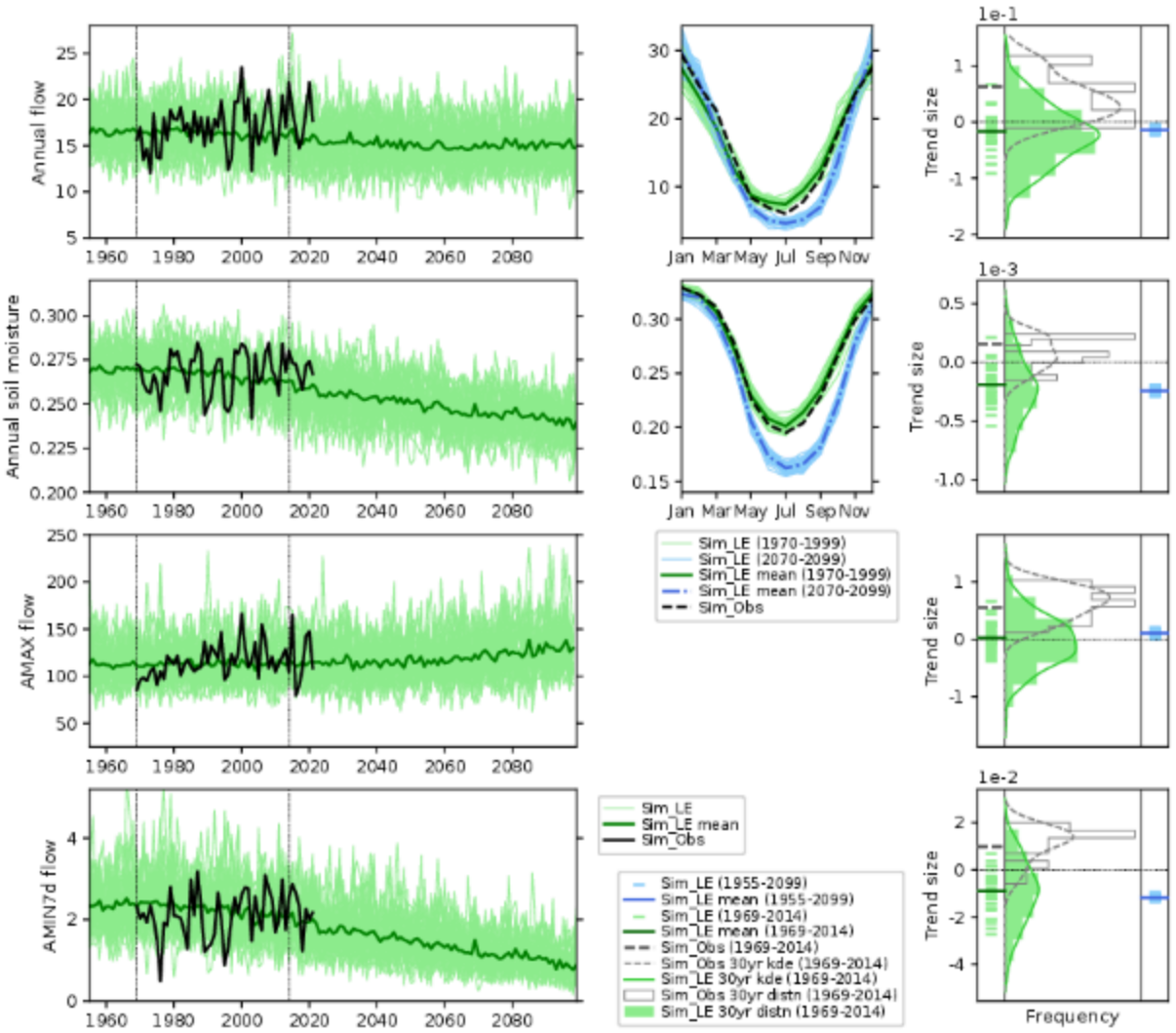



**Figure 3**

Time series of simulated GB-mean annual mean river flows, annual mean soil moisture, AMAX and AMIN7d for 1955-2099 (first column, top-to-bottom), with the monthly climatology of GB-mean flows and soil moisture in historical and far-future periods (second column), from Sim_LE (green lines), compared to Sim_Obs (black lines). Also shown are trends in each of the four variables (third column) for the historical period 1969-2014 for Sim_LE (green) and Sim_Obs (grey) and for the full period 1955-2099 for Sim_LE (blue). The latter plots show, as horizontal lines at the side, the individual trend sizes for each Sim_LE member for each period (short green/blue lines), the Sim_LE mean for each period (longer green/blue line), and Sim_Obs for the historical period (dashed black line). Also shown are the distributions of trend sizes derived from 30-year continuous sub-periods within 1969-2014 for each

Sim_LE member (green histogram with corresponding kernel density estimate) and Sim_Obs (grey histogram with corresponding kernel density estimate).

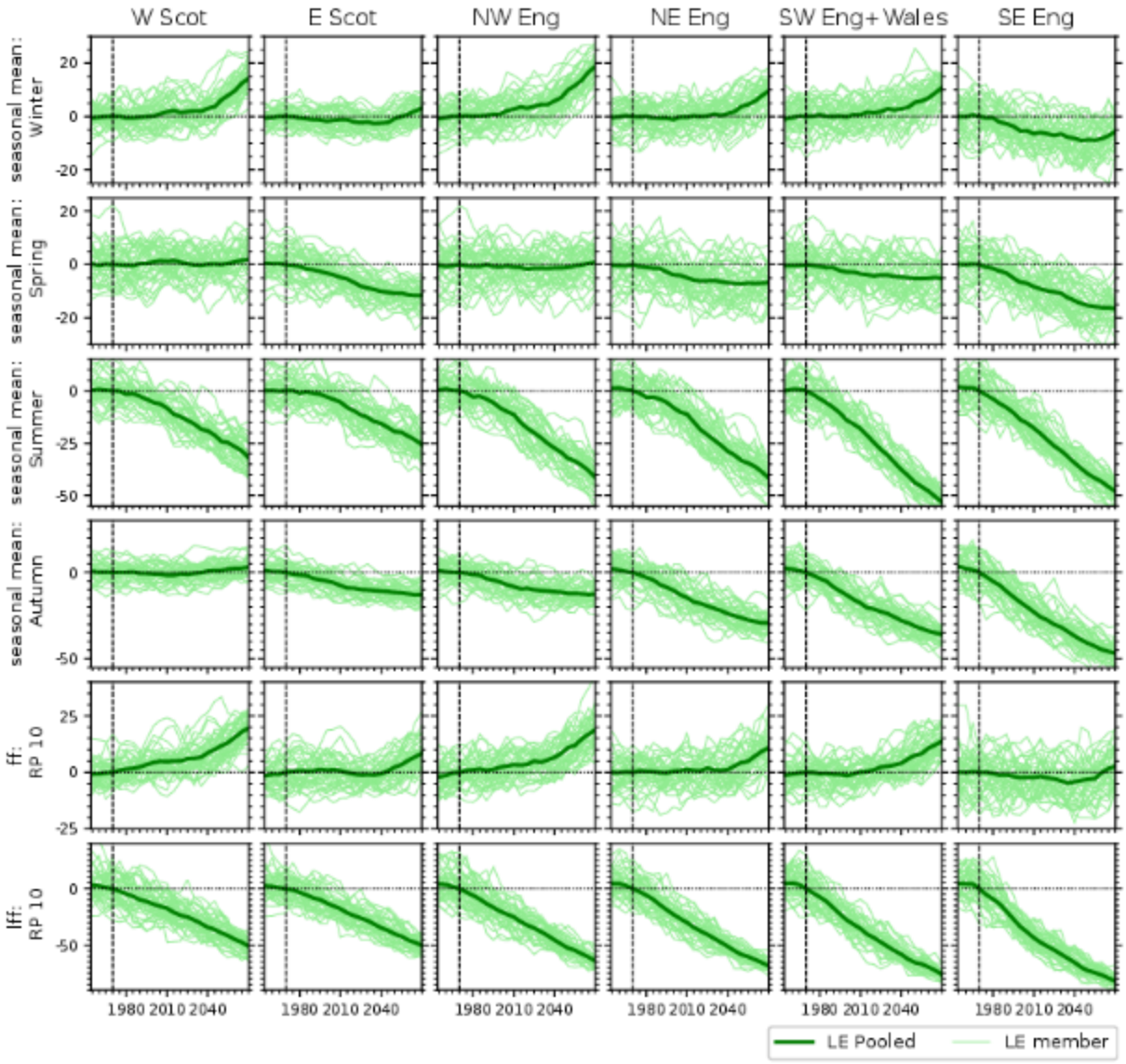



**Figure 4**

Time-series of changes in regional mean river flows, for 30-year periods between 1955-1984 and 2070-2099 moving forward 5 years at a time (relative to a pooled 1970-1999 baseline), for six regions (left-to-right) and the six flow indices (top-to-bottom).

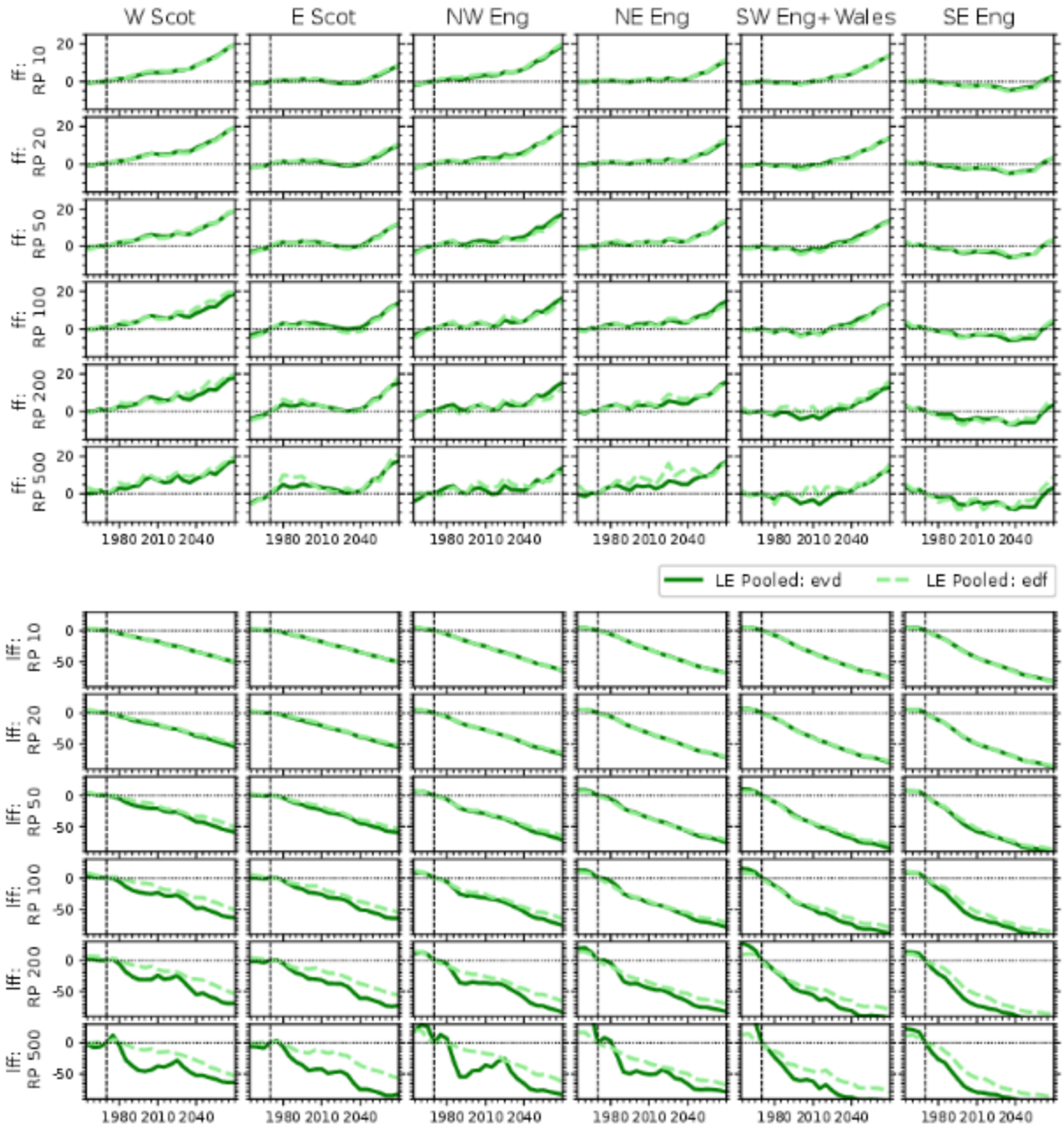



**Figure 5**

Time-series of changes in regional mean high flows (top 6 rows) and low flows (bottom 6 rows), calculated using fitted EVDs (solid lines) and empirical distributions (dashed lines) for 30-year periods between 1955-1984 and 2070-2099 moving forward 5 years at a time (relative to a pooled 1970-1999 baseline), for six regions (left-to-right). The returns periods in each case range for 10 to 500 years.

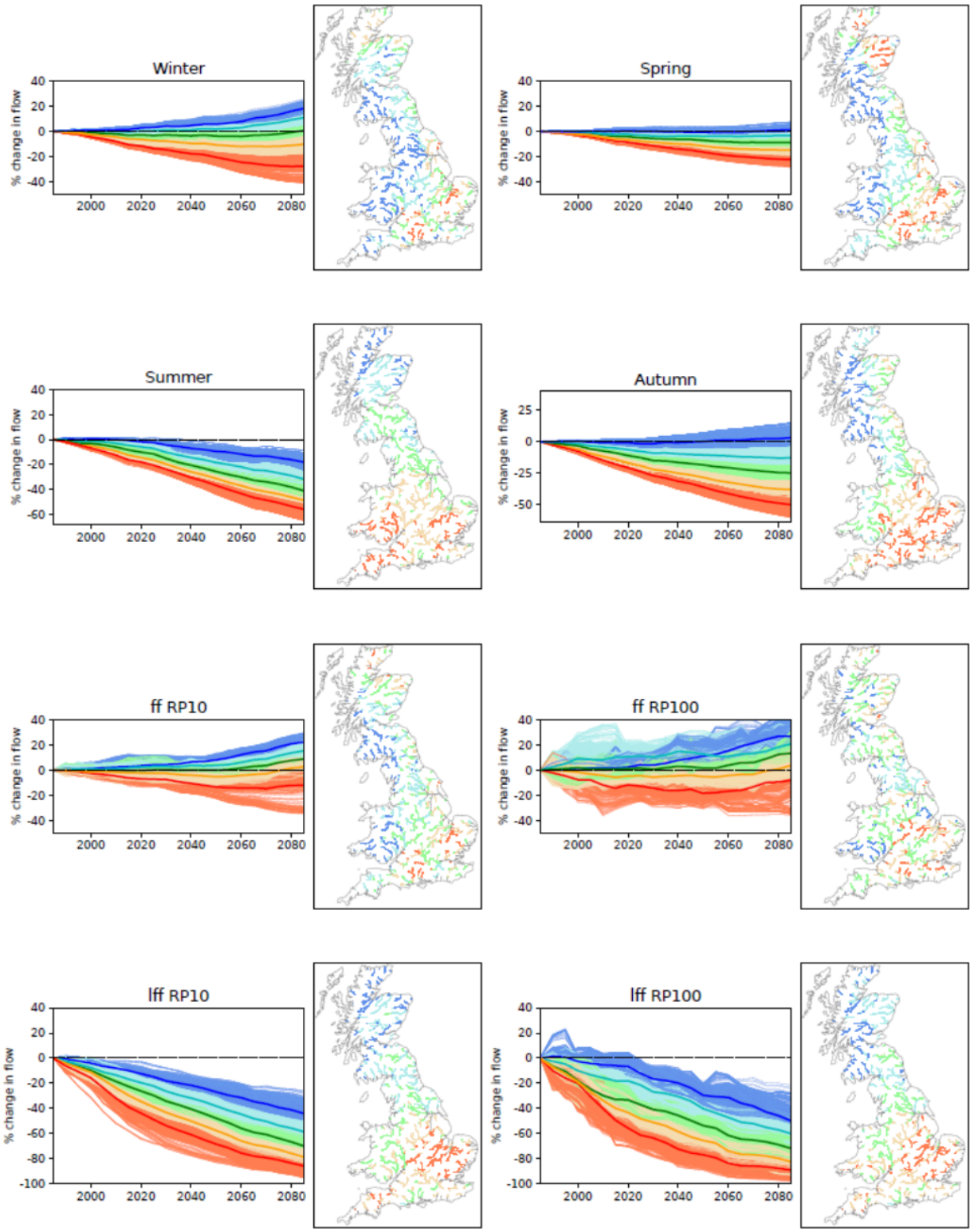



**Figure 6**

Clusters of river pixels (area ≥ 200km$^2$) with similar changes in flows for each season (top two rows), high flows (ff) with 10- and 100-year RPs (third row), and low flows (lff) with 10- and 100-year RPs (fourth row). The high and low flows are derived using empirical distributions.

# Supplementary Files

This is a list of supplementary files associated with this preprint. Click to download.

- G2GLEsetupandbroadscaleanalysesSuppMat.pdf